

# Computational Simulation of COX-1 (PDB: 3KK6) and COX-2 (PDB: 3LN1) Enzyme: 3D-QSAR Study, Docking Molecular and Simulation Dynamic on Series of Benzimidazole Derivatives

Rohit Jaysing Bhor\*, Saiprasad Vasant Wani, Kaushal Arjun Thorat, Omkar Balasaheb Sadaphal, Tanmay Rajendra Varpe, Prajwal Vijendra Ghogare, Shainesh Ganpat Bhosle, Sanket Sunilrao Gadekar

Department of Pharmaceutical Chemistry, Pravara Rural College of Pharmacy Pravaranagar, Rahata, Ahmednagar, Maharashtra, INIDA.

## ABSTRACT

**Background:** The proposed approach summarizes each activity *in silico* research. The structure-activity correlations and pharmacological effects of compounds containing benzimidazole are examined in this study. Using a variety of computational techniques, *in silico* studies allow for forecasting structural changes and how they would impact the pharmacological properties as well as the efficiency of these modifications. The computational study of benzimidazole derivatives is the main topic of this article. All compounds' cytotoxicity against inflammation was assessed, and the outcomes showed that several of them had strong inhibitions. **Materials and Methods:** The aim of this study was to investigate Cyclooxygenase-1 (COX-1) (PDB: 3KK6) and Cyclooxygenase-2 (COX-2) (PDB: 3LN1) enzyme inhibitory, and inflammatory activities of a new series of 1H-benzimidazole derivatives, for their possible use as multi-action therapeutic agents. Molecular Design Suite was used to conduct Combi Lab investigations and 3D-QSAR. Schrodinger Maestro was used for the molecular docking investigation. **Results:** Five compounds SW6; SW5; SW11; SW13 and SW15 in a library of 16 compounds created using a combinatorial approach demonstrated superior projected biological activity than the dataset's most active molecule. These chemicals exhibited proximal contact with amino acid residues on COX-2 (PDB: 3LN1) such as Phe381, Leu-384, Tyr-385, Trp-387, Phe-518, Gly-526, Met-522, Tyr348, Val-349, Leu-352. **Conclusion:** This study determined the structural elements affecting by carefully changing the substituents, ring modifications, and linker groups. The logical creation and optimization of more powerful and selective molecules is made possible by these discoveries. In contrast to the reference ligand, the current study produced more powerful benzimidazoles as inhibiting compounds for COX-1 (PDB: 3KK6) and COX-2 (PDB: 3LN1) with excellent interaction. The study's findings could aid in the creation of new COX-1 (PDB: 3KK6) and COX-2 (PDB: 3LN1) inhibitors to treat inflammatory conditions.

**Keywords:** Inflammation, ADMET, Benzimidazole, Molecular docking, COX-1 (PDB: 3KK6), COX-2 (PDB: 3LN1).

## Correspondence:

**Dr. Rohit Jaysing Bhor**

Department of Pharmaceutical Chemistry, Pravara Rural College of Pharmacy Pravaranagar, Rahata, Ahmednagar, Maharashtra, INIDA.  
Email: rohit.bhor69@gmail.com  
Orcid ID: 0000-0002-7979-3765  
Web of Science Researcher ID: GMX-4028-2022

**Received:** 27-02-2025;

**Revised:** 08-04-2025;

**Accepted:** 19-06-2025.

## INTRODUCTION

The exploration and subsequent synthesis of innovative hybrid molecules, characterized by a multifaceted array of pharmacological activities achievable through the modulation of a diverse spectrum of biochemical pathways, holds considerable promise in the therapeutic intervention of a wide range of pathological conditions, as it is well acknowledged that multifactorial disorders can have multiple origins.<sup>[1]</sup> Because the

hazards of drug-drug interactions are reduced, this approach has distinct advantages over drug combinations or multicomponent medications, notwithstanding the enormous difficulty in designing and optimizing such molecules. Atypical antipsychotics, such as olanzapine, risperidone, and aripiprazole, predominantly function as antagonists at dopamine and serotonin receptors, exhibiting a comparatively diminished affinity for histaminergic, cholinergic muscarinic, and  $\alpha$ -adrenergic receptor subtypes.<sup>[2]</sup> The synchronized combining of various advantageous moieties on similar substance, particularly for treatment of particular illness, is one of the promising developments in drug discovery.<sup>[3]</sup> The exordium for engendering avant-garde compounds exhibiting pleiotropic pharmacological effects resides optimally within the domain of pharmaceutical advantages that mitigate the exigency



ScienScript

DOI: 10.5530/ajbls.20251498

### Copyright Information :

Copyright Author (s) 2025 Distributed under Creative Commons CC-BY 4.0

Publishing Partner : ScienScript Digital, [www.scienscript.com.sg]

for polypharmacy, encompassing therapeutic modalities that concurrently attenuate iatrogenic sequelae, abrogate symptomatic manifestations, or potentiate salutary outcomes via adjuvant therapeutic mechanisms.<sup>[4]</sup>

Even if they have a lot of potential for therapeutic use, this is important to assess possibility of adverse consequences. High atomic weight is a common characteristic of dual inhibitors, which may lessen the likelihood of their therapeutic effects. Consequently, while designing dual inhibitors, the safety profiles and pharmacokinetic characteristics must be carefully taken into account.<sup>[5]</sup> The combination of imidazole with benzene results in the heterocyclic aromatic organic molecule known as benzimidazole. Because of their many effects, i.e., analgesic, anti-tumor, antiviral, and psychoactive properties, they have played a significant role in medicinal chemistry.<sup>[6]</sup> The intricate biological reaction of bodily tissues to infections, which is defensive action towards immune cells.<sup>[7]</sup> Cyclooxygenase (COX), which comes in the forms COX-1 (PDB: 3KK6) and COX-2 (PDB: 3LN1), is essential protein needed for convert arachidonic acid to prostaglandins. Prostaglandins are supplied by COX-1 (PDB: 3KK6) while COX-2 (PDB: 3LN1), is produced subsequent to inflammatory stimuli.<sup>[8]</sup> In human cancers, COX-2 (PDB: 3LN1) contributes to angiogenesis as well as cell division and death. One technique for figuring out how a protein and ligand interact is called molecular docking, and it explains the molecule's orientation, binding interactions, and binding energy.<sup>[9]</sup> Predicting the shared molecular characteristics those in molecular interactions with biological target and initiate response requires the use of pharmacophore methods.<sup>[10]</sup>

The purpose of this investigation was to determine the molecular interactions in benzimidazoles analogues and COX, as well as to screen the synthetic compounds' physicochemical and ADMET characteristics.<sup>[11]</sup> Additionally, pharmacophore modelling studies were used to examine distinctive traits. Since benzimidazole derivatives reported to have anti-inflammatory features, it is necessary to demonstrate how they work.<sup>[12]</sup> To ascertain these compounds *in silico* inhibitory effect, were docked with COX-1 (PDB: 3KK6) and COX-2 (PDB: 3LN1). As a result, *in silico* research helps identify how benzimidazoles work to block COX enzymes, which is what gives them their anti-inflammatory properties. Inflammation is a vital defensive mechanism against all forms of physical, chemical, and viral assault.<sup>[13]</sup> When this mechanism is dysregulated, the body develops pathological conditions, such as organ rejection, autoimmune diseases, and allergies.<sup>[14]</sup> Since NSAID show lowering fever, inflammation, and pain, millions of patients use them all over the world. NSAIDs function pharmacologically by blocking the actions of COX, which stops enzymatic biotransformation of arachidonic acid into related pro-inflammatory prostaglandins and Thromboxane (TXs).

Needleman and Isakson originally described two cyclooxygenase isoenzymes in 1997. The "House Keeping" enzyme, COX-1 (PDB: 3KK6) and COX-2 (PDB: 3LN1), regulates a basic level of PGs for homeostasis preservation, including intestinal integrity. The "Inducible" enzyme, COX-2, causes inflammatory reactions and is triggered by a variety of events. It is currently unclear what the exact roles of a COX-2 isoform that is solely expressed in particular brain and spinal cord areas are. The second COX type (COX-2) (PDB: 3LN1), produced in pathogenic and pro-inflammatory stimuli, including cytokines, lipopolysaccharides, and phorbol esters. COX2(PDB: 3LN1), is responsible for both PGs release and the inflammation. Numerous studies have linked COX-2 to a range of clinical illnesses, such as cancer, neurological disorders, and inflammation. As a result, also used in cancer treatment. In order to mitigate these serious side effects, selective COX-2 (PDB: 3LN1), inhibitor medications i.e, celecoxib, rofecoxib, and valdecoxib were created. These medications have analgesic property same as non-selective COX inhibitors, but they also have improved gastric safety profiles. Unfortunately, as they have adverse effects on COX pathway, which include an elevated risk of myocardial infarction and high blood pressure, valdecoxib and rofecoxib have both been removed from the market. The distinct chemical makeup of valdecoxib and rofecoxib was associated with their adverse effects. As a result, research for selective anti-inflammatory medications with superior safety profiles than the NSAIDs on the market is still ongoing. In COX-1 (PDB: 3KK6) and COX-2 (PDB: 3LN1), activity of inhibition synthesized derivatives was evaluated. Lastly, the synthesized compounds docked into COX2(PDB: 3LN1), site to clarify their possible method of action.

## MATERIALS AND METHODS

### Molecular Docking and Ligand preparation

Preceding molecular docking, test compounds SW1-SW16 structures and scheme of benzimidazole were given in Figure 1 and Table 1. We optimized by using the semi-empirical approach and the ArgusLab 4.0.1 software program. Getting proteins ready We used a variety of different COX-1 (PDB: 3KK6) and COX-2 (PDB: 3LN1), enzyme crystal structures via the RCSB for docking studies. Maestro 11.9 was used for all computational analysis. Software was installed on Dell Inc. 27-inch computer that was on Linux x86\_64 as OS and has Intel Core i7-7600U CPU at 3.90 GHz x8 with 16 GB RAM and 1 TB SSD. Drug likeness, physicochemical characteristics, and ADMET of compounds were studied. The PDB supplied Ribbon composition for COX-1 (PDB: 3KK6) and COX-2 (PDB: 3LN1). Auto dock version was 1.5.6. Chain A was chosen. Hydrogen with polarity and Gasteiger charges introduced after water was removed. They decided on a grid map. The compounds' 2D formula was drawn using ChemDraw Ultra 12.0. Avogadro software was used to minimize energy use. Autodock Vina was used to realize the docking process, while Discovery Studio 3.5 was used to

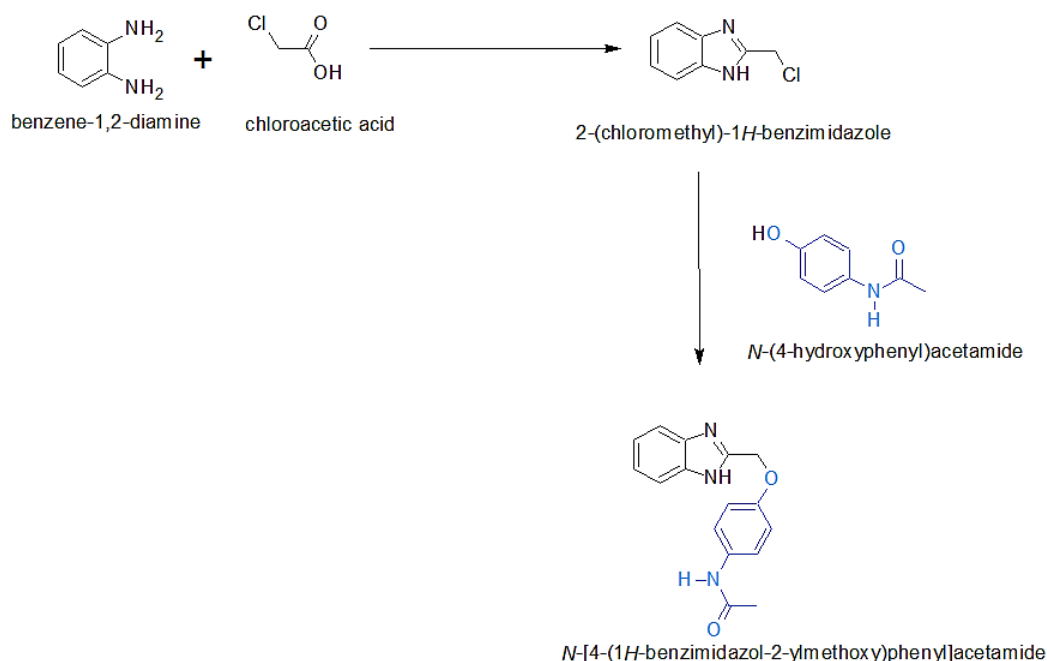
visualize the interactions. Celecoxib (CEL) crystal structures were compared to the anticipated conformations of docking data in order to optimize the docking method. Figure 2 showed the superimposition of the crystallized form of the Ribbon Structure Protein structure and Figure 3 showed Ramachandran Plot.

## RESULTS

### Molecular docking and Lipinski's rule of five

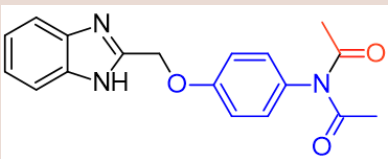
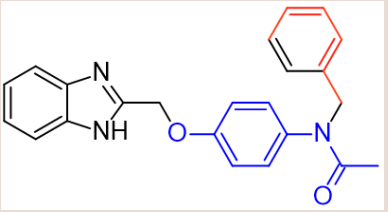
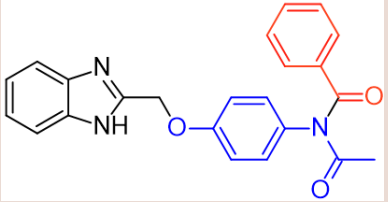
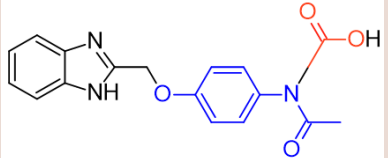
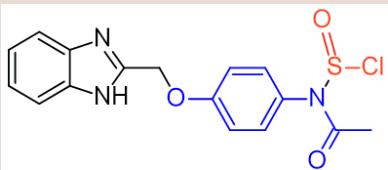
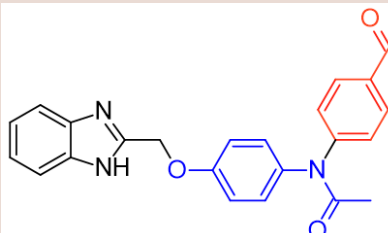
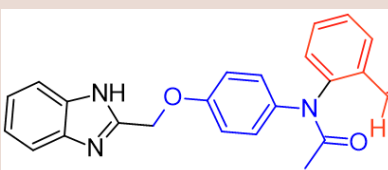
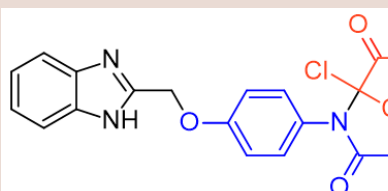
QSAR is one such technique that covered drug discovery in the above session/chapter. In this above session/chapter will cover the newly developed idea of "drug-likeness" as well as the computer modelling of several biological and physicochemical characteristics that are crucial in turning a clinical lead into a commercially available medication. Pharmacologists and medicinal chemists have looked for beneficial drug-like chemical characteristics that produce agents with predictable oral therapeutic effectiveness. Drug development process follows Lipinski's "rule of five" which is computational and experimental method for estimating solubility and permeability. COX-1 (PDB: 3KK6) and COX-2 (PDB: 3LN1) enzymes were docked with the drugs, and the molecular interactions between them were examined. Table 2 summarizes interactions between chemicals with residues of dynamic amino acids, whereas Figures 4 and 5 display the 2D - 3D conformations for molecular bindings. Computer-Aided Molecular Design (CAMD) has traditionally concentrated on lead optimization and identification, and several creative techniques have been created to help increase the binding affinities of drug candidates to certain receptors. Those are general guidelines which assess drug-likeness and

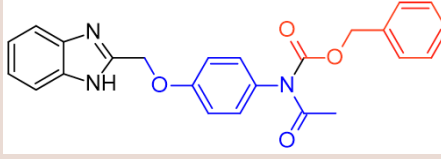
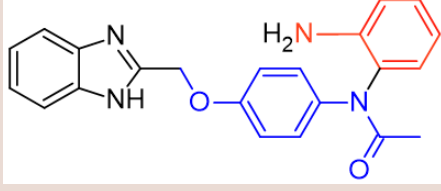
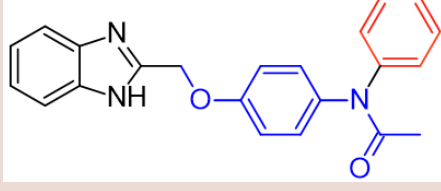
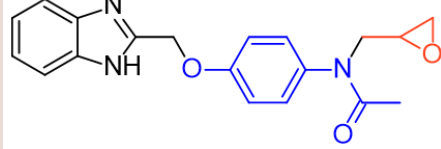
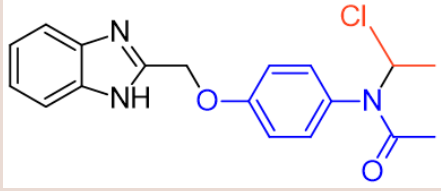
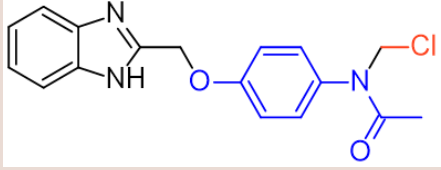
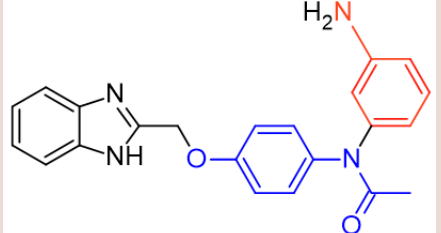
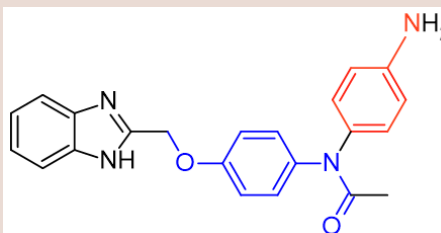
establish whether molecules have pharmacological activity. The rule was found on the finding that most medications that work well when taken orally are tiny, somewhat lipophilic molecules. It is employed in the process of developing new drugs when pharmacologically active lead structures are gradually improved to boost their activity and selectivity while maintaining their drug-like physicochemical characteristics. Bonds rotation; H-bond acceptors; H-bond donors; Lipinski; Ghose; Veber; Egan and Muegge violations were given in Table 3. ADMET (which stands for absorption, distribution, excretion, and toxicity) characteristics for substances are necessary to create effective oral medications. The toxicity of a ligand is thought to be required to ligand as function to effective discovery tool, and Qik-Prop produces physically relevant descriptions. The Ligprep module used for ligand preparation utilized in investigation. The protein preparation wizard is utilized for protein preparation. The PDB data bank provided the X-ray crystal structures of COX-1 (PDB: 3KK6) and COX-2 (PDB: 3LN1), The grid generated using Receptor Grid Generation Wizard. Receptor Grid Generation Wizard were given in Figure 6 Glide XP coupled the ligand with the protein, and the interactions were seen. Based on the optimal ligand-protein interaction, the scoring function assigns points. The extra-precision mode was used to assess the docking positions. The program detects steric conflicts, metal-ligation interactions, hydrophobic interactions, and hydrogen bonding. Every substance has a molecular weight between 400 and 500, which is less than 500. The compounds' computed log P values fall between 3.56-5.35. The substances being studied have donors of hydrogen bonds.



**Figure 1:** Scheme of Benzimidazole.

**Table 1: Derivatives of designed compound of Benzimidazole.**

| Comp. Code | Structure   |
|------------|---|
|            |    |
|            |    |
|            |    |
|            |   |
|            |  |
|            |  |
|            |  |
|            |  |

| Comp. Code | Structure   |
|------------|---|
|            |    |
|            |    |
|            |    |
|            |    |
|            |   |
|            |  |
|            |  |
|            |  |



### **In silico Admet**

Molecular modelling utilizes quantum techniques to evaluate the possibility of interaction, including cytochrome P450s, which has role in ADME processes. QSAR techniques is commonly used for data modelling. These look for relationships between a collection of chemical and structural molecules like GI absorption; BBB permeant; Pgp substrate; CYP1A2 inhibitor; CYP2C19 inhibitor; CYP2C9 inhibitor; CYP2D6 inhibitor; and CYP3A4 inhibitor in question and certain property using statistical methods. Choosing appropriate mathematical methods, appropriate chemical descriptors for ADMET endpoint, sizable enough collection of data pertaining with same endpoint for model validation are all essential components of effective prediction models for ADMET parameters. Good ADMET property prediction techniques are becoming more and more necessary to achieve two main goals. To lower the risk, novel compounds libraries should be designed first. Secondly, screening and testing should be optimized by focusing on the most promising compounds. Predicting characteristics like oral absorption, bioavailability, BBB penetration, clearance, and Vd (for frequency) which give information about dosage quantity and frequency is our goal. Molecular modelling and data modelling are the two categories of computational techniques that are employed. Recent developments in the prediction of ADME-related physicochemical qualities (like lipophilicity), ADME properties (like absorption), and toxicity problems (like drug-drug interactions) are discussed in this article see Table 4.

During the next ten years or so, automated medium and HTS *in vitro* tests will be employed.

### **DISCUSSION**

Analogues with best interactions and far from zero auto dock score determined as best conformation. Both complexes' Ramachandran Plot RMSD plot analysis revealed that the SW9-protein complex had a stable trajectory for more research after achieving excellent stability at 100 ns. Analysis of the synthetic benzimidazole derivatives. All of the "compounds had molecular weights less than 500," according to data warrior results, suggesting that they will bind action site. To have good *in vivo* response, pharmacodynamic and pharmacokinetic characteristics must be balanced. Further details on medication dose and regimen are also provided by ADMET. According to "Lipinski's rule of five", an oral medication is selected if its molecular weight is < 500, hydrogen bond donors is less than five, hydrogen bond acceptors is less than ten, and log P value less than five. Oral bioavailability depends on molecular flexibility, which is shown by the number of rotatable bonds. Additionally, as TPSA is indirectly related to percentage absorption, it suggested that it is used as 3D descriptor in number of hydrogen bonding groups. All drugs had LogP below 5, which indicates excellent penetration and absorption across cell membranes. Table provides various derivatives of benzimidazole which specifics on the "binding energies and hydrogen bonds" of SW1-SW16. Furthermore, the dock score values of all the produced compounds ranged from

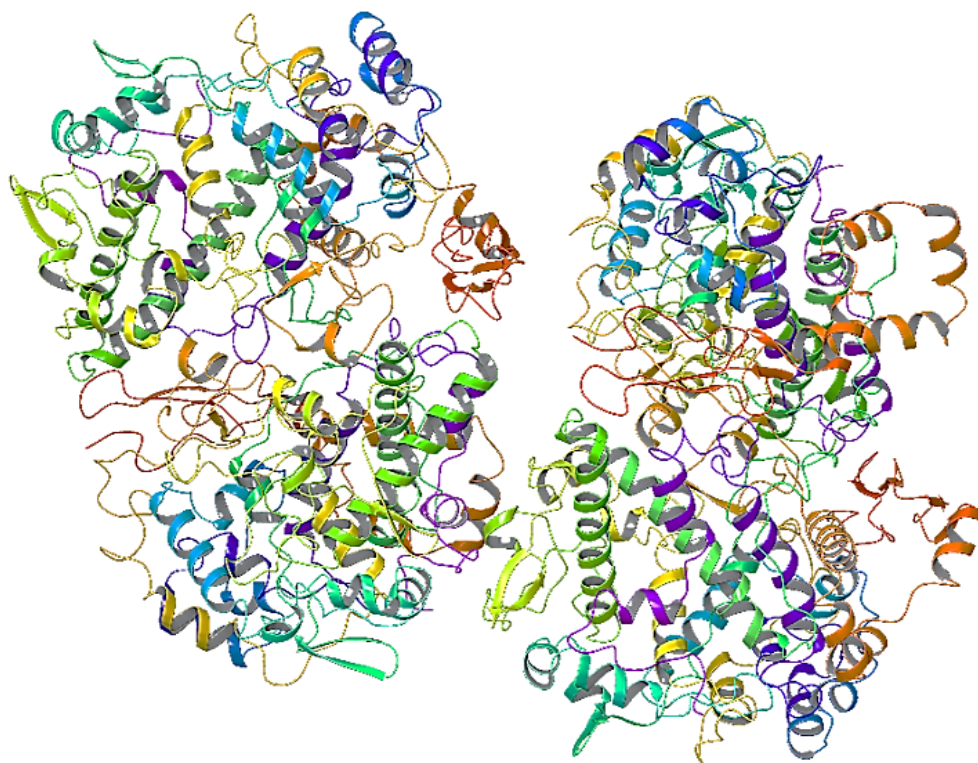


**Figure 2:** Ribbon Structure Protein structure.

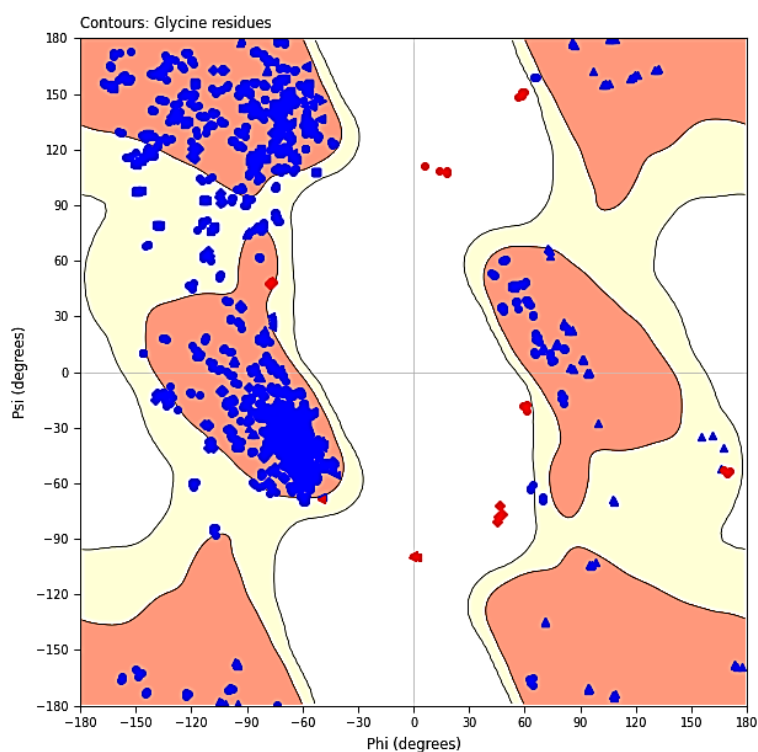


**Figure 3:** Ramachandran Plot.

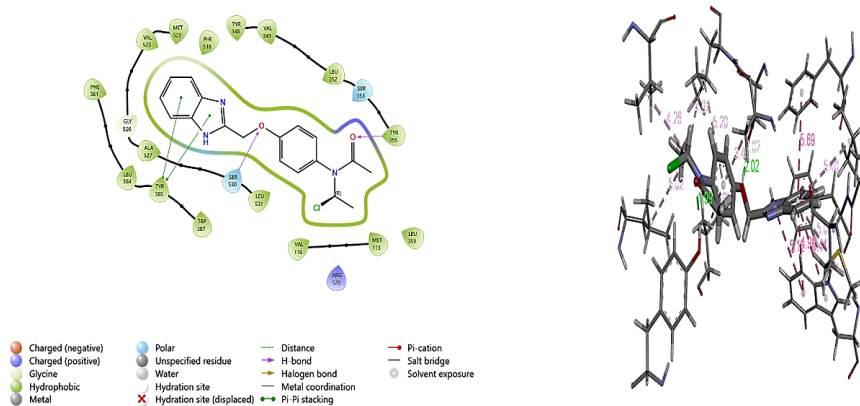


**Figure 4:** 2D and 3D conformations of the molecular bindings with Computer-aided molecular design (CAMD) of SW13.

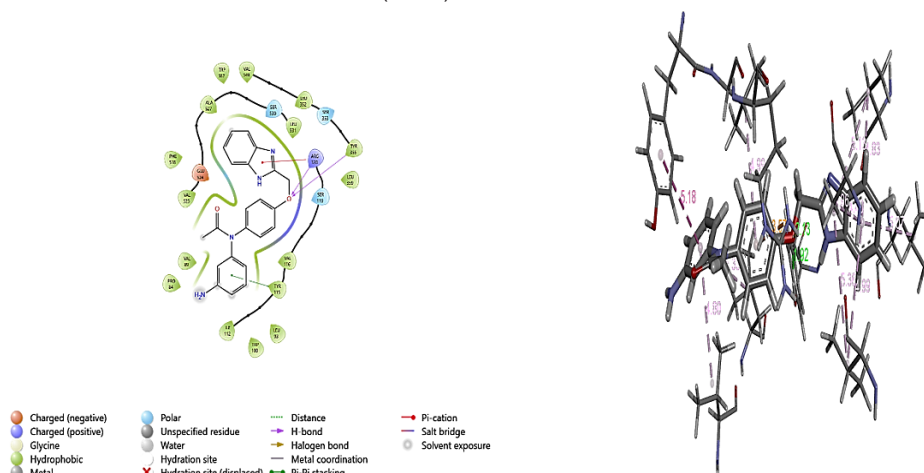


**Figure 5:** 2D and 3D conformations of the molecular bindings with Computer-aided molecular design (CAMD) of SW15.

**Table 2: Chemical interactions between the chemicals and the residues of active amino acids.**

| Name            | Distance | Category      | Type                       | Docking Score |
|-----------------|----------|---------------|----------------------------|---------------|
| SW5             |          |               |                            | -8.263        |
| TYR355:HH:      | 2.04716  | Hydrogen Bond | Conventional Hydrogen Bond |               |
| SER530:HG       | 1.97445  | Hydrogen Bond | Conventional Hydrogen Bond |               |
| SER530:HB1      | 2.9116   | Hydrogen Bond | Carbon Hydrogen Bond       |               |
| A:TYR355        | 5.86833  | Other         | Pi-Sulfur                  |               |
| PHE381          | 5.70974  | Hydrophobic   | Pi-Pi Stacked              |               |
| TYR385          | 4.68387  | Hydrophobic   | Pi-Pi T-shaped             |               |
| TRP387          | 4.89914  | Hydrophobic   | Pi-Pi T-shaped             |               |
| TRP387          | 5.20476  | Hydrophobic   | Pi-Pi T-shaped             |               |
| TRP387 -        | 5.45224  | Hydrophobic   | Pi-Pi T-shaped             |               |
| ALA527:N        | 4.47114  | Hydrophobic   | Amide-Pi Stacked           |               |
| ALA527:N        | 4.43481  | Hydrophobic   | Amide-Pi Stacked           |               |
| LEU384          | 5.42753  | Hydrophobic   | Pi-Alkyl                   |               |
| MET522          | 5.04609  | Hydrophobic   | Pi-Alkyl                   |               |
| VAL349          | 3.959    | Hydrophobic   | Pi-Alkyl                   |               |
| ALA527          | 3.49315  | Hydrophobic   | Pi-Alkyl                   |               |
| LEU531          | 5.15618  | Hydrophobic   | Pi-Alkyl                   |               |
| SW6             |          |               |                            | -8.387        |
| ARG120:HH12     | 2.28016  | Hydrogen Bond | Conventional Hydrogen Bond |               |
| ARG120:NH1      | 4.58916  | Electrostatic | Pi-Cation                  |               |
| LEU93           | 5.21572  | Hydrophobic   | Pi-Alkyl                   |               |
| VAL116          | 4.33303  | Hydrophobic   | Pi-Alkyl                   |               |
| VAL116          | 3.40784  | Hydrophobic   | Pi-Alkyl                   |               |
| VAL349          | 4.39845  | Hydrophobic   | Pi-Alkyl                   |               |
| ALA527          | 3.86229  | Hydrophobic   | Pi-Alkyl                   |               |
| LEU352          | 4.80044  | Hydrophobic   | Pi-Alkyl                   |               |
| SW11            |          |               |                            | -8.922        |
| ARG120:HH11 -   | 2.6146   | Hydrogen Bond | Conventional Hydrogen Bond |               |
| ARG120:HH12 - : | 2.70138  | Hydrogen Bond | Conventional Hydrogen Bond |               |
| A:TYR355:HH -   | 2.07332  | Hydrogen Bond | Conventional Hydrogen Bond |               |
| ARG120:NH1 -    | 3.04352  | Electrostatic | Pi-Cation                  |               |
| ARG120:NH1 -    | 4.01185  | Electrostatic | Pi-Cation                  |               |
| ARG120:NH2 -    | 3.7088   | Electrostatic | Pi-Cation                  |               |
| A:VAL89         | 4.82507  | Hydrophobic   | Pi-Alkyl                   |               |
| A:VAL116        | 4.83282  | Hydrophobic   | Pi-Alkyl                   |               |
| VAL349          | 5.05315  | Hydrophobic   | Pi-Alkyl                   |               |
| ALA527          | 3.52281  | Hydrophobic   | Pi-Alkyl                   |               |
| VAL349          | 5.17522  | Hydrophobic   | Pi-Alkyl                   |               |
| LEU352          | 5.48619  | Hydrophobic   | Pi-Alkyl                   |               |
| ALA527          | 4.71168  | Hydrophobic   | Pi-Alkyl                   |               |

| Name         | Distance | Category      | Type                       | Docking Score |
|--------------|----------|---------------|----------------------------|---------------|
| SW13         |          |               |                            | -8.471        |
| TYR355:HH    | 1.99025  | Hydrogen Bond | Conventional Hydrogen Bond |               |
| SER530:HG    | 2.02067  | Hydrogen Bond | Conventional Hydrogen Bond |               |
| SER530:HB1   | 3.02406  | Hydrogen Bond | Carbon Hydrogen Bond       |               |
| PHE381       | 5.69178  | Hydrophobic   | Pi-Pi Stacked              |               |
| TYR385       | 4.67032  | Hydrophobic   | Pi-Pi T-shaped             |               |
| TRP387       | 5.11958  | Hydrophobic   | Pi-Pi T-shaped             |               |
| TRP387       | 4.89984  | Hydrophobic   | Pi-Pi T-shaped             |               |
| TRP387 -     | 5.44236  | Hydrophobic   | Pi-Pi T-shaped             |               |
| VAL116       | 4.26357  | Hydrophobic   | Alkyl                      |               |
| LEU359       | 5.01817  | Hydrophobic   | Alkyl                      |               |
| LEU531       | 4.97275  | Hydrophobic   | Alkyl                      |               |
| LEU384       | 5.39901  | Hydrophobic   | Pi-Alkyl                   |               |
| MET522       | 5.03786  | Hydrophobic   | Pi-Alkyl                   |               |
| VAL349       | 3.94823  | Hydrophobic   | Pi-Alkyl                   |               |
| ALA527       | 3.49084  | Hydrophobic   | Pi-Alkyl                   |               |
| LEU531       | 5.19681  | Hydrophobic   | Pi-Alkyl                   |               |
| SW15         |          |               |                            | -8.157        |
| ARG120:HH11  | 2.12873  | Hydrogen Bond | Conventional Hydrogen Bond |               |
| TYR355:HH -  | 1.92239  | Hydrogen Bond | Conventional Hydrogen Bond |               |
| ARG120:NH1 - | 3.56621  | Electrostatic | Pi-Cation                  |               |
| TYR115       | 5.18484  | Hydrophobic   | Pi-Pi T-shaped             |               |
| VAL349       | 5.13415  | Hydrophobic   | Pi-Alkyl                   |               |
| VAL349       | 4.82907  | Hydrophobic   | Pi-Alkyl                   |               |
| LEU352       | 5.0732   | Hydrophobic   | Pi-Alkyl                   |               |
| VAL523       | 5.36067  | Hydrophobic   | Pi-Alkyl                   |               |
| VAL523       | 4.9863   | Hydrophobic   | Pi-Alkyl                   |               |
| ALA527       | 3.95758  | Hydrophobic   | Pi-Alkyl                   |               |
| ALA527       | 4.39767  | Hydrophobic   | Pi-Alkyl                   |               |
| VAL116       | 4.98707  | Hydrophobic   | Pi-Alkyl                   |               |
| VAL89        | 4.7953   | Hydrophobic   | Pi-Alkyl                   |               |
| LEU93        | 5.32878  | Hydrophobic   | Pi-Alkyl                   |               |

7.5 and 8.8 kcal/mol, suggesting their binding energies lower to benzimidazole, which has "binding energy" of 8.0 kcal/mol. Interactions towards COX-1 (PDB: 3KK6) and COX-2 (PDB: 3LN1) revealed that they have anti-inflammatory properties. Phe381, Leu-384, Tyr-385, Trp-387, Phe-518, Gly-526, Met-522, Tyr348, Val-349, Leu-352 were active amino acids in COX-1 (PDB: 3KK6) and COX-2 (PDB: 3LN1). SW5 and SW6 demonstrated Pi-Pi stacking to TYR355: HH; SER530:HG; SER530:HB1; TYR355; PHE381; TYR385; TRP387; TRP387; TRP387; ALA527:N; LEU384; MET522; VAL349; ALA527; and LEU531 via the benzimidazole and H-bond with Ser-530 via nitrogen of the benzimidazole ring. SW15 demonstrated Pi-Pi stacking with Tyr385 via the benzimidazole ring and hydrogen

bonding with Ser530. SW11 demonstrated Pi-Pi stacking with ARG120:HH11; ARG120:HH12; TYR355:HH; ARG120:NH1; ARG120:NH2; VAL89;VAL116;VAL349; ALA527;VAL349 and LEU352; ALA527 via benzene ring and H-bond with Met-522 via nitrogen. Comparing the 16 benzimidazole derivatives to the standard Indomethacin (- 10.705 kcal/mol), SW15 and SW11 had a satisfactory docking score of -8.572 kcal/mol. ARG120:HH11; ARG120:HH12; TYR355: HH; ARG120:NH1; ARG120:NH2; VAL89;VAL116;VAL349; ALA527;VAL349 and LEU352; ALA527, were active amino acids in the enzyme COX-1 (PDB: 3KK6) and COX-2 (PDB: 3LN1) enzymes. SW5 demonstrated H-Bond with TYR355: HH; SER530:HG; SER530:HB1; TYR355; PHE381; TYR385; TRP387; TRP387;



TRP387; ALA527:N; LEU384; MET522; VAL349; ALA527; and LEU531 nitrogen of benzimidazole and Pi-Pi stacking with Tyr-385 via benzene. SW13 demonstrated Pi-cation interaction to TYR355:HH; SER530:HG; SER530:HB1; PHE381; TYR385; TRP387; TRP387; TRP387; VAL116; LEU359; LEU531; LEU384; MET522; VAL349; ALA527 and LEU531 via benzimidazole and Pi-pi stacking with Tyr-385 and Trp-387 via benzene. SW9 demonstrated H-bond with ARG120:HH12; ARG120:NH1; LEU93; VAL116; VAL116; VAL349; ALA527; LEU352 and Ser-530 via benzimidazole and Pi-Pi stacking with Tyr-385. Comparing 16 benzimidazole derivatives to the standard Indomethacin (-10.099 kcal/mol), SW5, SW6, SW11, SW13 and SW15 showed elevated docking scores, from -8.25 to -8.51 kcal/mol. Compound SW5's binding affinity score with COX-1 (PDB: 3KK6) is -56.79 kcal/mol, whereas compound SW6's binding score with COX-2 (PDB: 3LN1) is -60.27 kcal/mol. Late-stage drug attrition may now be decreased, and the most promising compounds can be found using *in silico* ADME screens. They should thus have high oral absorption; nevertheless, this quality cannot be used to explain variances in bioactivity. Additionally, the compounds' oral absorption percentage ranged from 70.69 to 73.87%, indicating high ADME. Their TPSA values were 101.3 and 104.80 Å<sup>2</sup> (140 Å<sup>2</sup>), respectively, and rotatable bonds ranged in 7 to 8 (<10). It is generally accepted that a molecule that is soluble in water and satisfies Lipinski's and Veber's criteria is said to possess both lipophilicity and hydrophilicity. Interactions towards COX-1 (PDB: 3KK6) and COX-2 (PDB: 3LN1) enzymes revealed that they have anti-inflammatory properties. TYR355:HH; SER530:HG; SER530:HB1; TYR355; PHE381; TYR385;

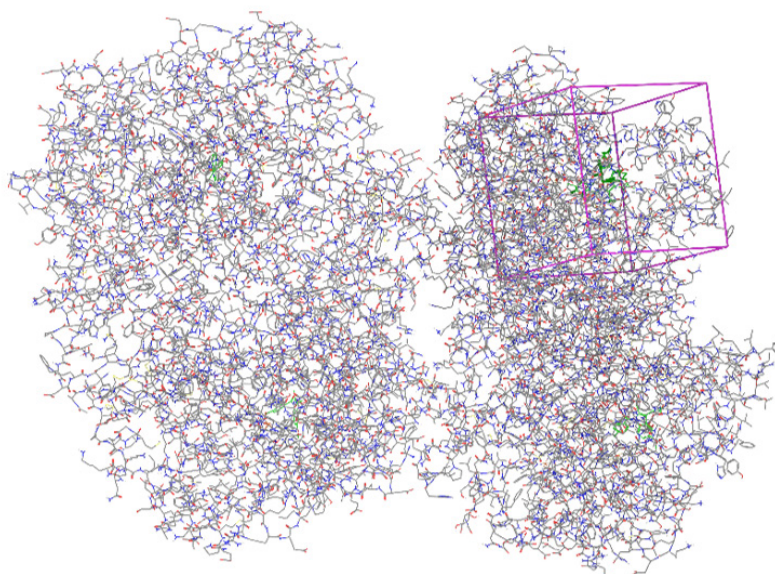
TRP387; TRP387; TRP387; ALA527:N; LEU384; MET522; VAL349; ALA527; and LEU531 were active amino acids in COX-1 (PDB: 3KK6) and COX-2 (PDB: 3LN1) enzymes. SW13 and SW15 demonstrated Pi-Pi stacking to Tyr385 and Trp387 via the benzimidazole and H-bond with Ser-530 via nitrogen of the benzimidazole ring. SW12 demonstrated Pi-Pi stacking with TYR355:HH; SER530:HG; SER530:HB1; TYR355; PHE381; TYR385; TRP387; TRP387; TRP387; ALA527:N; VAL349; ALA527; and LEU531 via the benzimidazole ring and hydrogen bonding with Ser530. SW14 demonstrated Pi-Pi stacking with Tyr-385 via benzene ring and H-bond with Met-522 via nitrogen. Comparing the 16 benzimidazole derivatives to the standard Indomethacin (-10.705 kcal/mol), SW14 and SW15 had a satisfactory docking score of -8.572 kcal/mol. Phe381, Leu384, Tyr385, Trp387, were active amino acids in the enzyme COX-1 (PDB: 3KK6) and COX-2 (PDB: 3LN1) enzymes. B15 demonstrated H-Bond with Ser-530 nitrogen of benzimidazole and Pi-Pi stacking with Tyr-385 via benzene. SW10 demonstrated Pi-cation interaction to TYR355:HH; SER530:HG; SER530:HB1; TYR355; PHE381; TYR385; TRP387; TRP387; TRP387; ALA527:N; LEU384; MET522; VAL349; ALA527; and LEU531 via benzimidazole and Pi-pi stacking with Tyr-385 and Trp-387 via benzene. SW1 demonstrated H-bond with TYR355:HH; SER530:HG; SER530:HB1; TYR355; PHE381; TYR385; TRP387; TRP387; TRP387; ALA527:N; LEU384; MET522; VAL349; ALA527; and LEU531 via benzimidazole and Pi-Pi stacking with Tyr-385. Comparing 16 benzimidazole derivatives to the standard Indomethacin (-10.099 kcal/mol), Late-stage drug attrition may now be decreased and the most promising

**Table 3: Rotatable bonds; H-bond acceptors; H-bond donors; Lipinski violations; Ghose violations; Veber violations; Egan violations and Muegge violations of Benzimidazole Derivatives.**

| Comp code | #Rotatable bonds | #H-bond acceptors | #H-bond donors | Lipinski #violations | Ghose #violations | Veber #violations | Egan #violations | Muegge #violations |
|-----------|------------------|-------------------|----------------|----------------------|-------------------|-------------------|------------------|--------------------|
| SW1       | 7                | 6                 | 2              | 1                    | 0                 | 1                 | 1                | 1                  |
| SW2       | 7                | 5                 | 2              | 0                    | 0                 | 0                 | 1                | 1                  |
| SW3       | 8                | 6                 | 2              | 1                    | 0                 | 1                 | 1                | 2                  |
| SW4       | 8                | 6                 | 2              | 0                    | 0                 | 0                 | 1                | 1                  |
| SW5       | 7                | 7                 | 2              | 1                    | 0                 | 1                 | 1                | 2                  |
| SW6       | 8                | 8                 | 3              | 1                    | 0                 | 1                 | 1                | 1                  |
| SW7       | 7                | 5                 | 3              | 1                    | 0                 | 1                 | 1                | 2                  |
| SW8       | 7                | 5                 | 3              | 1                    | 0                 | 1                 | 1                | 2                  |
| SW9       | 7                | 6                 | 2              | 0                    | 0                 | 0                 | 1                | 1                  |
| SW10      | 8                | 7                 | 2              | 1                    | 0                 | 1                 | 1                | 0                  |
| SW11      | 7                | 5                 | 2              | 0                    | 0                 | 0                 | 1                | 1                  |
| SW12      | 8                | 8                 | 3              | 1                    | 0                 | 1                 | 1                | 1                  |
| SW13      | 7                | 5                 | 2              | 0                    | 0                 | 0                 | 1                | 1                  |
| SW14      | 11               | 8                 | 2              | 1                    | 1                 | 2                 | 1                | 2                  |
| SW15      | 7                | 5                 | 2              | 0                    | 0                 | 0                 | 1                | 1                  |
| SW16      | 7                | 6                 | 2              | 0                    | 0                 | 0                 | 1                | 1                  |

**Table 4:** *In silico* ADMET of Benzimidazole derivatives.

| Molecule | GI absorption | BBB permeant | PGP substrate | CYP1A2 inhibitor | CYP2C19 inhibitor | CYP2C9 inhibitor | CYP2D6 inhibitor | CYP3A4 inhibitor | log Kp (cm/s) | Bioavailability Score |
|----------|---------------|--------------|---------------|------------------|-------------------|------------------|------------------|------------------|---------------|-----------------------|
| SW1      | High          | Yes          | Yes           | No               | No                | No               | No               | No               | -6.13         | 0.55                  |
| SW2      | High          | Yes          | Yes           | No               | Yes               | No               | Yes              | No               | -5.21         | 0.55                  |
| SW3      | High          | Yes          | Yes           | No               | Yes               | No               | No               | No               | -5.33         | 0.55                  |
| SW4      | High          | No           | Yes           | No               | No                | No               | No               | No               | -6.36         | 0.55                  |
| SW5      | High          | No           | No            | Yes              | Yes               | No               | Yes              | No               | -5.85         | 0.55                  |
| SW6      | High          | No           | Yes           | No               | Yes               | No               | Yes              | No               | -5.63         | 0.55                  |
| SW7      | High          | No           | Yes           | No               | Yes               | No               | Yes              | No               | -5.63         | 0.55                  |
| SW8      | High          | No           | Yes           | Yes              | Yes               | No               | No               | No               | -5.9          | 0.55                  |
| SW9      | High          | No           | Yes           | No               | Yes               | Yes              | No               | No               | -5.34         | 0.55                  |
| SW10     | High          | No           | Yes           | No               | Yes               | No               | Yes              | No               | -5.65         | 0.55                  |
| SW11     | High          | Yes          | Yes           | No               | Yes               | No               | Yes              | No               | -5.07         | 0.55                  |
| SW12     | High          | Yes          | Yes           | No               | Yes               | No               | Yes              | No               | -6.28         | 0.55                  |
| SW13     | High          | Yes          | Yes           | No               | Yes               | No               | Yes              | No               | -5.3          | 0.55                  |
| SW14     | High          | Yes          | Yes           | No               | Yes               | No               | Yes              | No               | -5.52         | 0.55                  |
| SW15     | High          | No           | Yes           | No               | Yes               | No               | Yes              | No               | -5.65         | 0.55                  |
| SW16     | High          | No           | Yes           | No               | Yes               | No               | Yes              | No               | -5.65         | 0.55                  |

**Figure 6:** Receptor Grid Generation Wizard.

compounds can be found using *in silico* ADME screens. To have a good *in vivo* response, pharmacodynamic and pharmacokinetic characteristics must be balanced. Further details on medication dose and regimen are also provided by ADMET.

## CONCLUSION

The ligands SW15 and SW13 had high docking scores with COX-1 (PDB: 3KK6) enzymes (-9.492 kcal/mol) and COX-2 (PDB: 3LN1) (-8.572 kcal/mol), respectively, out of the 16 benzimidazole derivatives. Furthermore, the pharmacophoric

characteristics that underlie their biological action were also disclosed. As a result, these *in silico* methods have helped identify binding and affinity between COX enzyme and benzimidazoles, responsible for anti-inflammatory properties. To ascertain their anti-inflammatory properties, benzimidazole analogues were docked with COX-1 (PDB: 3KK6) and COX-2 (PDB: 3LN1) enzymes. All of the compounds' values were discovered to be within the typical range, and Lipinski's rule of five was not broken. Therefore, it is anticipated that the compounds will have a high oral bioavailability.

## ACKNOWLEDGEMENT

The authors are thankful to Dr. S.B. Bhawar, Pravara Rural College of Pharmacy, Pravaranagar.

## CONFLICT OF INTEREST

The authors declare that there is no conflict of interest.

## ABBREVIATIONS

**mg/kg:** Milligram/kilograms; **sec:** Seconds; **kcal:** Kilocalorie; **Mol. Wt:** Molecular Weight; **g:** Gram; **LEU:** Leucine; **THR:** Threonine; **ALA:** Alanine; **MET:** Methionine; **PHE:** Phenylalanine; **COX:** Cyclooxygenase Enzyme; **WHO:** World Health Association; **Log P:** Partition Coefficient.

## ETHICAL APPROVAL

No Ethical Approval (*In vitro* Activity).

## REFERENCES

- Cuadrado, A., and Nebreda, A. R. Mechanisms and functions of p38 MAPK signalling. *Biochemical Journal*, 2010; 429(3): 403-17. <https://doi.org/10.1042/bj20100323>
- Rathod, R., Amrita Khair, Kale, A., and Joshi, S. A combined supplementation of vitamin B12 and n-3 polyunsaturated fatty acids across two generations improves nerve growth factor and vascular endothelial growth factor levels in the rat hippocampus. *Neuroscience*, 2016; 339: 376-84. <https://doi.org/10.1016/j.neurosci.2016.10.018>
- Field, M. S., Kamynina, E., Chon, J., and Stover, P. J. Nuclear folate metabolism. *Annual Review of Nutrition*, 2018; 38(1): 219-43. <https://doi.org/10.1146/annurev-nutr-071714-034441>
- Gröber, U., Kisters, K., and Schmidt, J. Neuroenhancement with Vitamin B12-Underestimated Neurological Significance. *Nutrients*, 2013; 5(12): 5031-45. <https://doi.org/10.3390/nu5125031>
- Hobbenaghi, R., Javanbakht, J., Hosseini, E., Mohammadi, S., Rajabian, M., Moayeri, P., *et al.* RETRACTED ARTICLE: Neuropathological and neuroprotective features of vitamin B12 on the dorsal spinal ganglion of rats after the experimental crush of sciatic nerve: an experimental study. *Diagnostic Pathology*, 2013; 8(1). <https://doi.org/10.1186/1746-1596-8-123>
- Chan, W., Almasieh, M., Catrinescu, M., and Levin, L. A. Cobalamin-Associated superoxide scavenging in neuronal cells is a potential mechanism for vitamin B12-Deprivation optic neuropathy. *American Journal of Pathology*, 2017; 188(1): 160-72. <https://doi.org/10.1016/j.ajpath.2017.08.032>
- Horiuchi, K., Amizuka, N., Takeshita, S., Takamatsu, H., Katsuura, M., Ozawa, H., *et al.* Identification and Characterization of a Novel Protein, Periostin, with Restricted Expression to Periosteum and Periodontal Ligament and Increased Expression by Transforming Growth Factor  $\beta$ . *Journal of Bone and Mineral Research*, 1999; 14(7): 1239-49. <https://doi.org/10.1359/jbmr.1999.14.7.1239>
- Boehm, J. C., Smietana, J. M., Sorenson, M. E., Garigipati, R. S., Gallagher, T. F., Sheldrake, P. L., *et al.* 1-Substituted 4-Aryl-5-pyridinylimidazoles: A New Class of Cytokine Suppressive Drugs with Low 5-Lipoxygenase and Cyclooxygenase Inhibitory Potency. *Journal of Medicinal Chemistry*, 1996; 39(20): 3929-37. <https://doi.org/10.1021/jm960415o>
- Ben-Levy, R., Hooper, S., Wilson, R., Paterson, H. F., and Marshall, C. J. Nuclear export of the stress-activated protein kinase p38 mediated by its substrate MAPKAP kinase-2. *Current Biology*, 1998; 8(19): 1049-57. [https://doi.org/10.1016/S0960-9822\(98\)70442-7](https://doi.org/10.1016/S0960-9822(98)70442-7)
- Lee, J. C., and Young, P. R. Role of CSBP/p38/RK stress response kinase in LPS and cytokine signaling mechanisms. *Journal of Leukocyte Biology*, 1996; 59(2): 152-7. <https://doi.org/10.1002/jlb.59.2.152>
- Ono, K., and Han, J. The p38 signal transduction pathway Activation and function. *Cellular Signalling*, 2000; 12(1): 1-13. [https://doi.org/10.1016/S0898-6568\(99\)00071-6](https://doi.org/10.1016/S0898-6568(99)00071-6)
- Kumar, S., Boehm, J., and Lee, J. C. p38 MAP kinases: key signalling molecules as therapeutic targets for inflammatory diseases. *Nature Reviews Drug Discovery*, 2003; 2(9): 717-26. <https://doi.org/10.1038/nrd1177>
- Ramesh, G. Novel therapeutic targets in neuroinflammation and neuropathic pain. *Inflammation and Cell Signaling*. 2014. <https://doi.org/10.14800/ics.111>
- Streit, W. J., Mrak, R. E., and Griffin, W. S. T. Microglia and neuroinflammation: a pathological perspective. *Journal of Neuroinflammation*, 2004; 1(1): 14. <https://doi.org/10.1186/1742-2094-1-14>

**Cite this article:** Bhor RJ, Wani SV, Thorat KA, Sadaphal OB, Varpe TR, Ghogare PV, *et al.* Computational Simulation of COX-1 (PDB: 3KK6) and COX-2 (PDB: 3LN1) Enzyme: 3D-QSAR Study, Docking Molecular and Simulation Dynamic on Series of Benzimidazole Derivatives. *Asian J Biol Life Sci.* 2025;14(2):x-x.